arXiv:cond-mat/0306088v1 [cond-mat.str-el] 4 Jun 2003

# The Orbital Order Parameter in $La_{0.95}Sr_{0.05}MnO_3$ probed by Electron Spin Resonance

J. Deisenhofer,[1] B.I. Kochelaev,[2] E. Shilova,[2] A.M. Balbashov,[3] A. Loidl,[1] and H.-A. Krug von Nidda[1]

[1] *Experimentalphysik V, Center for Electronic Correlations and Magnetism, Institute for Physics, Augsburg University, D-86135 Augsburg, Germany*
[2] *Kazan State University, 420008 Kazan, Russia*
[3] *Moscow Power Engeneering Institute, 105835 Moscow, Russia*

(Dated: February 6, 2008)

The temperature dependence of the electron-spin resonance linewidth in $La_{0.95}Sr_{0.05}MnO_3$ has been determined and analyzed in the paramagnetic regime across the orbital ordering transition. From the temperature dependence and the anisotropy of linewidth and $g$-value the orbital order can be unambiguously determined via the mixing angle of the wave functions of the $e_g$-doublet. The linewidth shows a similar evolution with temperature as resonant x-ray scattering results.

PACS numbers: 77.22.Gm, 64.70.Pf

In transition-metal oxides the orbital degrees of freedom play an important role for the electric and magnetic properties. Their coupling to spin, charge and lattice is responsible for the occurrence of a variety of complex electronic ground states. Orbital order (OO) can be derived via the Jahn-Teller (JT) effect or via superexchange (SE) between degenerate orbitals under the control of strong Hund's-rule coupling [1]. Strong correlations exist between spin and orbital order and between OO and lattice distortions, but of course a one-to-one correspondence cannot be expected. While spin and lattice order can easily be detected experimentally, this is not true for OO and so far the OO parameter remains hidden. In recent years resonant x-ray scattering (RXS) has been used to derive information on the OO parameter [2], but there is an ongoing dispute, whether RXS probes the JT distortion or the orbital charge distribution [3, 4]. Indirectly, OO can also be derived from diffraction experiments via lattice distortions and bond lengths [5]. In this Letter we demonstrate that electron-spin resonance (ESR) can be used to detect OO and to monitor the evolution of the OO parameter. Probing the spin of the partially filled $d$-shell of $Mn^{3+}$ ions by ESR, the anisotropy and $T$-dependence of $g$-value and linewidth $\Delta H$ provide clear information on OO via spin-orbit (SO) coupling.

The power of ESR to gain insight into OO will be demonstrated on A-type antiferromagnetic (AFM) $LaMnO_3$ ($T_N$=140 K), the parent compound of the magneto-resistance manganites and a paradigm for a cooperative JT effect that suggests a $d_{3x^2-r^2}/d_{3y^2-r^2}$-type OO below $T_N$=750 K [6]. However, it has been shown that SE interactions play an important role, too [7]. Several recent studies exhibit clear anomalies of the ESR parameters at the JT transition in both doped and pure $LaMnO_3$ [8, 9, 10, 11]. The orbitally ordered $O'$-phase is characterized by an anisotropy of $\Delta H$ [11, 12], which for polycrystalline samples reduces to a broad maximum in $\Delta H(T)$ [9, 10]. Previously, the angular dependencies of $\Delta H$ and the resonance field $H_{res}$ had been analyzed for 200 K and 300 K in high-temperature approximation, allowing to estimate the Dzyaloshinsky-Moriya (DM) interaction and the strength of the zero-field splitting (ZFS) parameters [13]. At X-Band frequencies (9 GHz) $\Delta H$ was of the same order of magnitude as $H_{res}$ and due to the overlap with the resonance at $-H_{res}$ and their mutual coupling via the nondiagonal elements of the dynamic susceptibility [14] the values for $H_{res}$ contained a rather large uncertainty. To avoid these problems we performed new experiments at Q-band frequencies (34 GHz), which allowed a better determination of $H_{res}$.

The scope of the present paper is the comprehensive analysis of the $T$-dependence and anisotropy of $\Delta H$ and the $g$-value of the ESR signal in $La_{0.95}Sr_{0.05}MnO_3$. We chose this concentration for the present study as an untwinned single crystal was available and $T_{JT}\sim$605 K is accessible to our experimental setup [15].

New ESR measurements were performed with a Bruker ELEXSYS E500 CW spectrometer at Q-Band frequencies ($\nu \approx$ 34 GHz, 4.2 K $\leq T \leq$ 290 K), using a continuous gas-flow cryostat for He (Oxford). The oriented sample was mounted in a quartz tube with paraffin. A goniometer allowed the rotation of the sample around an axis perpendicular to the static magnetic field $\vec{H}_{ext}$.

Figure 1 shows $\Delta H$ for X-band frequency and Fig. 2 $\Delta H$ and the effective $g$-value $g_{eff}=h\nu/(\mu_B H_{res})$ determined from $H_{res}$ for Q-band frequency. The observed linewidths at both frequencies nicely coincide. Only near the minimum below 200 K the absolute values are slightly enhanced at 34 GHz as compared to 9 GHz. Whereas the $g$-values obtained at X-band frequency bear a rather large uncertainty [11, 13], at Q-band frequency the $g$-values show a regular $T$-dependence, approaching a constant high-temperature value and increasing for $T \rightarrow T_N$. First, we determined the ZFS parameters $D$ and $E$ from the $T$ dependence of $H_{res}$ at Q-band frequency. Using the general formula for the resonance shift due to crystal field (CF) effects [13, 16] and accounting only for the rotation (angle $\gamma$) of the $MnO_6$ octahedra in the $ac$ plane (axis notation like in Ref. 17), we obtained the following expressions for the effective $g$-values for $\vec{H}_{ext}$ applied

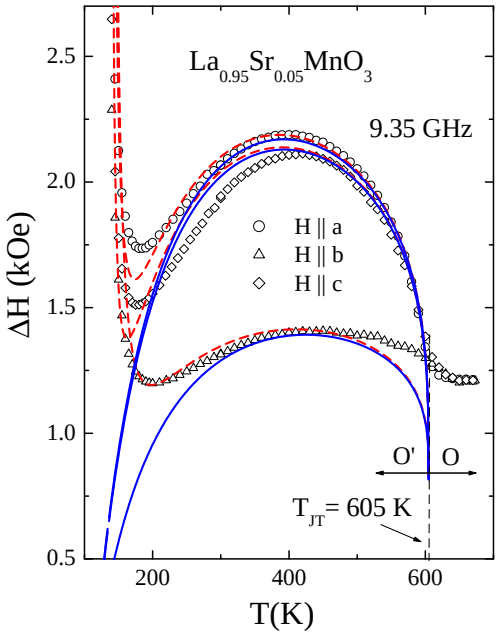


FIG. 1: $\Delta H(T)$ in $La_{0.95}Sr_{0.05}MnO_3$ at X-Band frequency for $\vec{H}_{\rm ext}$ applied parallel to the three main axes of the orthorhombic structure. Solid and dashed lines represent fits using eq. (2) as described in the text.

along one of the crystallographic axes

$$\frac{g^{\rm eff}_{a,c}(T)}{g_{a,c}} \approx 1 + \frac{D}{T-T_{\rm CW}}\left[(3\zeta-1) \pm 3(1+\zeta)\sin(2\gamma)\right]$$
$$\frac{g^{\rm eff}_{b}(T)}{g_{b}} \approx 1 - \frac{2D}{T-T_{\rm CW}}(3\zeta-1), \qquad (1)$$

with the Curie-Weiss (CW) temperature $T_{\rm CW}$ and $\zeta = E/D$. All terms of second and higher order in $D/(T - T_{\rm CW})$ were neglected. The $T$-dependence of the effective $g$-values is, hence, given by the CW law of the magnetic susceptibility. Excluding the critical regime on approaching magnetic order below 170 K, the data are well described by this approach (solid lines in Fig. 2), where $T_{\rm CW}$ was kept fixed at 111 K [11]. The rotation angle was chosen as $\gamma$=13° as observed in pure $LaMnO_3$ [5, 17]. Then all data can be consistently described by $D = 0.60(2)$ K, the $E/D$-ratio $\zeta$=0.37(1), and the $g$-values $g_a$=1.988(1), $g_b$=1.986(1), and $g_c$=1.984(1). From these crystallographic $g$-values, the local $g$ values of $Mn^{3+}$ can be calculated as $g_z$=1.977, $g_y(=g_b)$=1.986, and $g_x$=1.995, typical for ions with less than half-filled $3d$-shell with the longest and shortest Mn-O bond along the local $z$ and $x$ direction, respectively [18].

The main result of this evaluation is the $E/D$-ratio, which we improved in comparison to our previous estimate [13] by the Q-band experiment. For $\vec{H}_{\rm ext}$ applied along the $b$-axis the data are nearly $T$-independent, whereas they clearly exhibit the CW behavior for the other orientations. Regarding the equation for $g_b$, this is only possible, if the factor $(3\zeta - 1)$ is close to zero and hence $\zeta \approx 1/3$. This result is independent on the value of the rotation angle $\gamma$. Only the absolute value of $D$ directly depends on the choice of $\gamma$, which accounts for the splitting of the resonance fields between $a$ and $c$ direction.

With the obtained $E/D$-ratio we now turn to the evaluation of the linewidth data. A detailed derivation of the CF contributions to the ESR linewidth in the cooperative JT distorted perovskite structure accounting for the mutual rotations of the $MnO_6$ octahedra is presented in Ref. 19. These theoretical considerations can be summarized in the following formula

$$\Delta H^{(\vartheta,\varphi)}(T) = \frac{T-T_{\rm CW}}{T}[\Gamma_{\rm DM}(\infty) + \qquad (2)$$
$$+ \left(1-\frac{T}{T_{\rm JT}}\right)^{2\beta}(\Gamma_{\rm CF}(\infty) f^{(\vartheta,\varphi)}_{\rm reg}$$
$$+ \Gamma_{\rm CFD}\left(\frac{T_{\rm N}}{6(T-T_{\rm N})}\right)^{\alpha} f^{(\vartheta,\varphi)}_{\rm div})],$$

where the first term describes the contribution $\Gamma_{\rm DM}(\infty)$ of the DM interaction as introduced by Huber et al. [8] assuming that the exchange constants are $T$-independent. This contribution is expected to survive the JT transition and hence to determine the line broadening also at $T > T_{\rm JT}$. The second and third term, $\Gamma_{\rm CF}$ and $\Gamma_{\rm CFD}$, represent the regular and divergent CF contributions, respectively. Only the latter diverges for $T \to T_{\rm N}$ with an exponent $\alpha$, whereas both terms decrease for $T \to T_{\rm JT}$ with a critical exponent $2\beta$, with $\beta$ being the critical exponent of the ZFS parameters $D$ and $E$. Note that both the assumption of $T$ independent exchange constants and the application of the criticality at $T_{\rm JT}$ throughout the entire paramagnetic $O'$-phase can influence the value of the critical exponent $\beta$ which therefore has to be regarded cautiously. The angular factors $f^{(\vartheta,\varphi)}_{\rm reg}$ and $f^{(\vartheta,\varphi)}_{\rm div}$ read

$$f^{(\vartheta,\varphi)}_{\rm reg} = f_{\rm div} + (1+\zeta)^2(1+\frac{3}{2}\sin^2\vartheta),$$
$$f^{(\vartheta,\varphi)}_{\rm div} = \frac{1}{2}[1-3\zeta+2\gamma(1+\zeta)]^2(1-\sin^2\vartheta\sin^2\varphi)$$
$$+ \frac{1}{2}[1-3\zeta-2\gamma(1+\zeta)]^2(1-\sin^2\vartheta\cos^2\varphi),$$

where $\vartheta$ and $\varphi$ are the polar and azimuthal angles between $\vec{H}_{\rm ext}$ and the crystallographic $b$ and $c$ axes, respectively. An analogous calculation to the one presented in [19] showed that the DM interaction does not exhibit any critical behavior at $T_{\rm N}$. To minimize the number of fit parameters, we neglected here any angular dependence of the DM contribution. In first approximation this is justified by the observation that above $T_{\rm JT}$ the linewidth is isotropic. However, generally an anisotropy of the DM contribution can arise in the orbitally ordered state [13]. But it consists itself at least in two contributions from different Mn-O-Mn bond geometries, and

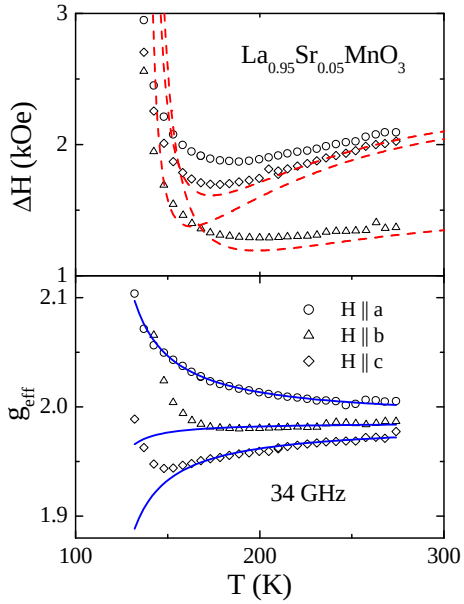


FIG. 2: $\Delta H(T)$ and effective g-value $g_{\rm eff}(T)$ at Q-band frequency for $\vec{H}_{\rm ext}$ applied parallel to the three crystallographic axes of the orthorhombic structure. The solid lines represent fits using eq. (1) for $g_{\rm eff}$, the dashed lines for $\Delta H$ are the same as in Fig. 1.

its transformation to an isotropic behavior on approaching $T_{\rm JT}$ needs further theoretical considerations. In the minimal model we omitted the divergent CF contribution ($\Gamma_{\rm CFD}$=0) and tried to find the best fit for the linewidth data. The characteristic temperatures were kept fixed at $T_{\rm CW}$=111 K and $T_{\rm JT}$=605 K and the rotation angle in the $ac$ plane was set to $\gamma$=13°. In addition the parameter $\zeta$=0.37 was taken from the evaluation of the $g$-values. So only three fit parameters remain, as there are the regular part of the CF contribution $\Gamma_{\rm CF}(\infty)$, its critical exponent $\beta$ at the JT transition, and the DM contribution $\Gamma_{\rm DM}(\infty)$, which survives also at temperatures $T > T_{\rm JT}$. A simultaneous fit (solid lines in Fig. 1) of the $T$-dependence of $\Delta H$ is satisfactorily performed above 200 K with $\Gamma_{\rm DM}(\infty)$=1.0(1) kOe, $\Gamma_{\rm CF}(\infty)$=0.57(2) kOe, and $\beta$=0.16(1).

Finally, we added the effect of the divergent CF contribution, which allows to increase the difference between $\Delta H_a$ and $\Delta H_c$ to lower temperatures, as observed in the experiment. As shown in Fig. 1 (dashed lines) a satisfactory qualitative description of the data was obtained by $\Gamma_{\rm CFD}$=10 kOe and $\alpha$=1.8 with fixed $T_N$=135 K. Comparison with the Q-band data Fig. 2 indicates that the magnetic critical exponent below 200 K rather turns to the theoretically expected lower value of $\alpha$=0.75 [19], which however is not applicable at higher temperatures. The reason is that the fit function is used for the whole temperature range, but the derivation of the power law only holds for temperatures close to $T_{\rm N}$. A further improvement may be achieved by taking into account the symmetric anisotropic exchange interaction, which is beyond the scope of this paper. In the following we concentrate on the information obtained from the regular part of $\Delta H$.

The DM contribution $\Gamma_{\rm DM}(\infty)$=1.0 kOe determined in the $O'$-phase is lower than the one expected from $\Delta H\approx$1.4 kOe in the $O$-phase. This discrepancy can be explained by linewidth contributions of the CF due to the dynamic JT effect present in the $O$-phase [20]. Comparison with the regular CF contribution $\Gamma_{\rm CF}(\infty)$=0.57 kOe allows to estimate the averaged value $D_{\rm DM}$ of the DM interaction as defined in Ref. 8. The ratio of the linewidth contributions equals the ratio of the respective second moments approximated by $10(D_{\rm DM}/D)^2\approx\Gamma_{\rm DM}(\infty)/\Gamma_{\rm CF}(\infty)$ [8]. With $D$=0.6 K one obtains $D_{\rm DM}\approx$0.25 K. These values are free from the uncertainty in the estimation of the exchange frequency in the exchange-narrowed linewidth [19], because we used the $g$-values to determine the absolute values. They are smaller than the values estimated earlier for polycrystalline $LaMnO_3$ but their relative strength is in good agreement with previous results [8, 9].

After having extracted the ZFS parameters we will now discuss the consequences for OO in $LaMnO_3$:
In Fig. 3(a) the reduced ESR linewidth $\Delta H_a\cdot T/(T - T_{\rm CW})$ for $\vec{H}_{\rm ext}$ parallel to the $a$-axis, which bears the critical behavior on approaching $T_{\rm JT}$ (see eq. 2), and the RXS intensity obtained by Murakami *et al.*[2] for $LaMnO_3$ are shown to visualize the similarity of the two quantities on approaching both $T_{\rm N}$ and $T_{\rm JT}$. Note that we used the fixed value $T_{\rm CW}$=111 K of the $O'$-phase leading to somewhat lower values for the $O$-phase. It has been pointed out that the RXS intensity close to $T_{\rm JT}$ is $\propto(1-T/T_{\rm JT})^{2\beta}$ [4], where $\beta$ denotes the critical exponent of the OO parameter given by the pseudo spin $\vec{T}$=1/2(sin Θ, 0, cos Θ) [4, 23]. The angle Θ=2arctan($c_2/c_1$) is a measure of the mixing of the wave functions of the $e_g$-doublet in the ground state $\psi_g=c_1|3z^2-r^2\rangle+c_2|x^2-y^2\rangle$. To compare the results of RXS and ESR we fitted the RXS data in the vicinity of the JT transition (650 K$\leq T\leq T_{\rm JT}$=780 K) with such a critical behavior (solid line in Fig. 3(a)) and obtained an exponent $\beta$ = 0.16(1) in agreement with the ESR linewidth. Considering that the ZFS parameters can be denoted as $D=-3(\rho+\lambda^2/\Delta)\cos\Theta$ and $E=-\sqrt{3}(\rho+\lambda^2/\Delta)\sin\Theta$ with the spin-spin coupling $\rho$, the SO coupling $\lambda$ and the $t_{2g}$-$e_g$ splitting energy $\Delta$ [18], it is easy to identify the relation with the OO parameter $\vec{T}$. Despite the lack of data in the critical regime, Fig. 3(b) shows the orbital mixing coefficents $c_1$ and $c_2$ determined from a neutron diffraction (ND) study by Rodriguez-Carjaval *et al.* [5] The dashed lines were obtained by using $K(1-T/T_{\rm JT})^{\beta/2}+2^{-1/2}$ ($T_{\rm JT}$=750 K) with a critical exponent $\beta/2$ provided by $D\propto(c_1^2-c_2^2)$ and $E\propto c_1\cdot c_2$. With $K_1$=0.10 and $K_2$=-0.12 the data for $c_1$ and $c_2$ can be well described throughout the JT distorted phase. However, attempting to describe the three

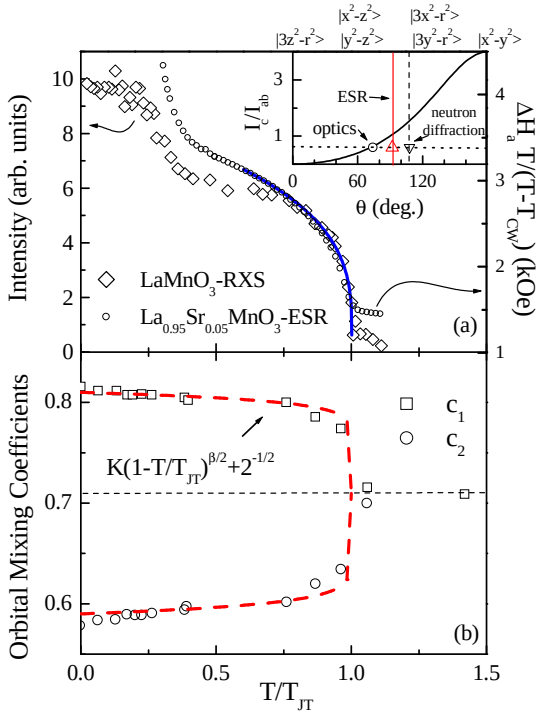


FIG. 3: $T$-dependence of (a) the reduced ESR linewidth in $La_{0.95}Sr_{0.05}MnO_3$ compared to the RXS intensity of $LaMnO_3$ taken from [2]. The solid line is a fit of the RXS intensity as described in the text. Inset: $\Theta$-dependence of the normalized optical spectral weight $I_c/I_{ab}$ following [21] (solid line) with the experimentally derived $\Theta$-values; (b) $T$-dependence of $c_1$ and $c_2$ determined by ND taken from [5]. The dashed lines were obtained using $K(1-T/T_{\rm JT})^{\beta/2}+2^{-1/2}$.

data points in the critical regime rather suggest $\beta\sim0.3$. Only a detailed structural study in the critical regime will allow a direct confirmation of the critical exponent for $c_1$ and $c_2$, but $\beta/2=0.08$ seems to yield a reasonable description.

The main result of this study is to estimate the angle $\Theta=\sqrt{3}\arctan(E/D)$ and determine the type of OO by using the obtained value $E/D=0.37(1)$, which after taking into account the transformation to a local coordinate system [19] results in $\Theta_{\rm ESR}\sim92°$. Another estimate has been obtained from ND via the orbital mixing coefficents at room temperature $c_1\approx 0.8$ and $c_2\approx0.6$ resulting in $\Theta_{\rm ND}=106°$ [5]. This discrepancy cannot easily be explained. However, Tobe *et al.* tried to explain the anisotropy of the optical conductivity in $LaMnO_3$ on the basis of a $p-d$ transition model by using the ratio $I_c/I_{ab}=2(1-\cos\Theta)/(2+\cos\Theta)$ (see inset of Fig. 3(a)) between the optical spectral weight with the polarization within the ferromagnetic (FM) plane (there $ab$) and along the AFM axis (there $c$).[21] Their simple model suggests a value $\Theta\sim74°$ to describe the experimental value of $I_c/I_{ab}=0.6$ at 10 K in the AFM regime. Theoretically, only a slight decrease of $\Theta$ below $T_{\rm N}$ is expected [7, 22] and therefore above $T_{\rm N}$ $\Theta_{\rm ESR}\sim92°$ yields a better description of the anisotropic properties of $LaMnO_3$ in the orbitally ordered state than $\Theta_{\rm ND}\sim106°$. Alejandro *et al.* derived a similar $E/D$-value from ESR data in $La_{7/8}Sr_{1/8}MnO_3$ [12] which confirms our result. To the best of our knowledge no $\Theta$-estimate has been obtained by RXS and it is worthwhile to note that the RXS intensity becomes maximal for $\Theta=\pi/2$ [4], the value obtained by ESR. Following [23] $\Theta=\pi/2$ characterizes OO stabilized by the SE processes in the FM bonds and the electron-phonon coupling is small compared to the bandwidth. Recent calculations suggest $\Theta=\pi/2$ at $T=T_{\rm N}$ and $\Theta=83°$ at $T=0$ and confirm our findings [22].

In summary, we were able to determine unambiguously the orbital order of $La_{0.95}Sr_{0.05}MnO_3$. The evolution of the OO parameter monitored by the RXS intensity shows an intriguing similarity to the ESR linewidth. We found a mixing angle $\Theta=92°$ suggesting that OO is dominated by SE coupling in agreement with theoretical predictions.

We thank M.V. Eremin, T. Kopp, and K.-H. Höck for fruitful discussions. This work was supported by the BMBF under contract No. 13N6917 (EKM) and partly by the DFG via the SFB 484 and DFG/RFFI-project No. 436-RUS 113/566/0. B.I.K. and E.S. were partially supported by CRDF via grant REC-007.

[1] H.A. Jahn and E. Teller, Proc. R. Soc. London **161**, 220 (1937); K.I. Kugel and D.I. Khomskii, Sov. Phys. Usp. **25**, 231 (1982).
[2] Y. Murakami *et al.*, Phys. Rev. Lett. **81**, 582 (1998).
[3] P. Benedetti *et al.*, Phys. Rev. B **63**, 060408 (2001).
[4] S. Ishihara *et al.*, Rep. Prog. Phys. **65**, 561 (2002).
[5] J. Rodriguez-Carvajal *et al.*, Phys. Rev. B **57**, R3189 (1998).
[6] J.B. Goodenough, Phys. Rev. **100**, 564 (1955).
[7] S. Okamoto *et al.*, Phys. Rev. B **65**, 144403 (2002).
[8] D.L. Huber *et al.*, Phys. Rev. B **60**, 12155 (1999).
[9] M. Tovar *et al.*, Phys. Rev. B **60**, 10199 (1999).
[10] J. Deisenhofer *et al.*, Phys. Rev. B **66**, 054414 (2002).
[11] V.A. Ivanshin *et al.*, Phys. Rev. B **61**, 6213 (2000).
[12] G. Alejandro *et al.*, Physica B **320**, 26 (2002); private communication.
[13] J. Deisenhofer *et al.*, Phys. Rev. B **65**, 104440 (2002).
[14] H. Benner *et al.*, J. Phys. C **16**, 6011 (1983).
[15] M. Paraskevopoulos *et al.*, J. Phys.: Condens. Matter **12**, 3993 (2000); A. Pimenov *et al.*, Phys. Rev. B **62**, 5685 (2000).
[16] N.O. Moreno *et al.*, Phys. Rev. B **63**, 174413 (2001).
[17] Q. Huang *et al.*, Phys. Rev. B **55**, 14987 (1997).
[18] A. Abragam and B. Bleaney, *Electron Paramagnetic Resonance of Transition Ions*, (Clarendon, Oxford, 1970).
[19] B. I. Kochelaev *et al.*, to be published.
[20] M.C. Sánchez *et al.*, Phys. Rev. Lett. **90**, 045503 (2003).
[21] K. Tobe *et al.*, Phys. Rev. B **64**, 184421 (2001).
[22] O. Sikora *et al.*, Acta Phys. Pol. B **34**, 861 (2003).
[23] R. Maezono *et al.*, Phys. Rev. B **58**, 11583 (1998).